

Hierarchical models for small area estimation using zero-inflated forest inventory variables: comparison and implementation

Grayson W. White^{1,2,*}, Andrew O. Finley^{1,2}, Josh K. Yamamoto³, Jennifer
L. Green², Tracey S. Frescino⁴, David W. MacFarlane¹, and Hans-Erik
Andersen⁵

¹Department of Forestry, Michigan State University, East Lansing, MI, USA

²Department of Statistics & Probability, Michigan State University, East Lansing, MI, USA

³Redcastle Resources, Inc., Salt Lake City, UT, USA

⁴Rocky Mountain Research Station, USDA Forest Service, Riverdale, UT, USA

⁵Pacific Northwest Research Station, USDA Forest Service, Seattle, WA, USA

*Corresponding author: Grayson W. White, whitegra@msu.edu

Abstract

National Forest Inventory (NFI) data are typically limited to sparse networks of sample locations due to cost constraints. While traditional design-based estimators provide reliable forest parameter estimates for large areas, there is increasing interest in model-based small area estimation (SAE) methods to improve precision for smaller spatial, temporal, or biophysical domains. SAE methods can be broadly categorized into area- and unit-level models, with unit-level models offering greater flexibility—making them the focus of this study. Ensuring valid inference requires satisfying model distributional assumptions, which is particularly challenging for NFI variables that exhibit positive support and zero inflation, such as forest biomass, carbon, and volume. Here, we evaluate a class of two-stage unit-level hierarchical Bayesian models for estimating forest biomass at the county-level in Washington and Nevada, United States. We compare these models to simpler Bayesian single-stage and two-stage frequentist approaches. To assess estimator performance, we employ simulated populations and cross-validation techniques. Results indicate that small area estimators that incorporate a two-stage approach to account for zero inflation, county-specific random intercepts and residual variances, and spatial random effects provide the most reliable county-level estimates. We illustrate the usefulness of simulated populations and cross-validation for assessing qualities of the various estimators considered.

Keywords: model-based estimation, Gaussian processes, Bayesian, forest biomass, simulation study

1 Introduction

National Forest Inventories (NFIs) play a critical role in collecting data and monitoring forest trends to assess resource availability, health, composition, and other economic and ecological attributes across various spatial scales within a given country. In the United States, the NFI is conducted by the United States Department of Agriculture (USDA) Forest Service through the Forest Inventory and Analysis (FIA) Program. Traditionally, NFIs such as FIA have been designed to provide precise estimates at broader spatial scales, such as state-level assessments of forest attributes like timber volume and biomass. However, there is growing interest among data users, along with increased funding, in obtaining more precise biomass estimates at finer spatial scales, such as the county-level (Prisley et al., 2021; Wiener et al., 2021; U.S. Senate, 2023). This rising demand, coupled with the widespread availability of high-resolution remote sensing data, has prompted researchers to develop and apply innovative small area estimation (SAE) methods that integrate FIA and similar NFI data with remote sensing products (Cao et al., 2022; May et al., 2023; Finley et al., 2024).

Despite the wide variety of SAE methods, they can generally be categorized into two main approaches: area-level and unit-level methods (Rao and Molina, 2015). Both aim to estimate the same parameter of interest but differ significantly in their use of data. In area-level modeling, survey unit response variable measurements are aggregated at each area. These aggregates are referred to as direct estimates and are typically generated using a design-based estimator. Direct estimates are then set as the area-level response variable in a regression model that might include area-level summaries of predictor variables and structured random effects. The goal of areal models is to use sources of auxiliary information to smooth noisy direct estimates. In contrast, unit-level approaches retain response variable measurements at the individual unit level. Set as the response variable, these unit-level measurements are coupled with spatial and/or temporally aligned predictor variables, possibly along with structured random effects, in a predictive model. This predictive model is then used to predict for all unobserved units. Finally, predictions are aggregated to any user-defined area

of interest.

The advantages and trade-offs of SAE approaches have only begun to be explored in the forest inventory literature. Area-level modeling often benefits from a more linear relationship between response and predictor variables and does not require precise plot locations, which is particularly useful given that NFI plot locations are often confidential. However, aggregation leads to data loss, limits the ability to model fine-scale (i.e., unit-level) relationships, precludes delineation of new areas of interest after model fitting, and imposes statistical assumptions that might be difficult to justify. For example, in the classical area-level Fay-Herriot model, within-area variance of the direct estimate is assumed to be fixed and known, although in practice it is estimated from limited data (Fay and Herriot, 1979; Rao and Molina, 2015). These variances enter the area-level model through a random effect, often without strong theoretical justification or consistency between the two inferential paradigms (see, e.g., Shannon et al., 2024, for discussion). In contrast, unit-level approaches leverage precise plot locations to model fine-scale spatial relationships more effectively, making them particularly valuable when such data are available.

Unlike design-based estimators, which derive their properties from the sampling design, model-based estimators rely entirely on the assumed data-generating process and the selection of an appropriate model. As a result, particular care must be taken in specifying SAE models and conducting rigorous model checking. One of the most effective approaches to evaluating SAE models is through the use of simulated populations that closely mimic the true—but only partially observed—population of interest. Simulated populations enable us to examine how inference varies under different conditions (e.g., varying sample sizes) and to compare our estimates against “true” values. To ensure that this evaluation is meaningful, it is essential to generate simulated populations using processes that are not closely aligned with the models under assessment.

Beyond assessment using simulated populations, we can evaluate models through cross-validation using observed data (e.g., leave-one-out or k -fold cross-validation). However, in

SAE studies, the primary parameters of interest exist at the area level. Unit-level models can be assessed using cross-validation at the unit level (i.e., iteratively holdout one or more observations, predict for those holdout, and compare the predictions to the holdout true values); however, we must be careful to verify the unit-level assessments align with how well the estimator performs once predictions are aggregated to the desired areas of interest.

This study evaluates a range of unit-level SAE approaches for estimating average biomass at the county level in Washington and Nevada. A key challenge in this context arises when estimating biomass across areas with a mix of forest and non-forest landcover. Specifically, biomass values exhibit a mixture of continuous positive values and true zeroes, a phenomenon referred to here as “zero-inflation.” While the term zero-inflation is commonly used in the statistical literature to describe a discrete distribution with an excessive number of zeros, in this case, biomass follows a continuous distribution with an additional zero component. Various model-based approaches have been developed to address zero-inflation in SAE. Notably, Pfeiffermann et al. (2008) introduced a two-stage mixture model to account for zero-inflation in the response variable, exploring both frequentist and Bayesian modes of inference. Their findings suggest that mean squared error (MSE) estimation is more straightforward in the Bayesian paradigm due to the advantages of Markov chain Monte Carlo (MCMC) simulation in uncertainty propagation across the model stages. Expanding on this work, Chandra and Sud (2012) applied the same two-stage model in a frequentist setting and introduced a parametric bootstrap-based MSE estimator.

In forest inventory applications, zero-inflation has received relatively limited attention. Finley et al. (2011) developed a two-stage model for zero-inflation in continuous forest attributes such as biomass, volume, and age, employing a hierarchical Bayesian framework with Gaussian process-based spatial random effects. Their approach enables unit-level predictions of forest attributes along with uncertainty quantification, though they did not directly produce small area estimates. More recently, White et al. (2025) applied the zero-inflated SAE model from Chandra and Sud (2012) to FIA data in Nevada, generating county-level biomass

estimates. Their study compared the zero-inflated estimator to other commonly used small area estimators, including estimators based on the Battese-Harter-Fuller unit-level model and the Fay-Herriot area-level model (Fay and Herriot, 1979; Battese et al., 1988). Their simulation results indicate the zero-inflated estimator improves point estimates and produces competitive MSE estimates, though further refinements remain possible (see Figure 2 in White et al., 2025).

In this study, we compare and extend model-based SAE approaches that account for zero-inflation, applying them to FIA data and remote sensing products for Washington and Nevada, as described in Section 2.1. Specifically, we evaluate nine model-based approaches, including the zero-inflated estimator from Chandra and Sud (2012) and eight hierarchical Bayesian estimators of increasing complexity. These Bayesian estimators include both single-stage models that do not explicitly address zero-inflation and two-stage models designed to account for a preponderance of zeros. With state counties defining our small areas of interest, we investigate the effects of incorporating county-varying intercepts, county-varying coefficients, county-specific residual variances, and spatially-varying intercepts. Section 2.3 provides further details on these models. Rather than defaulting to the most complex estimator, we sequentially introduce additional model components and evaluate their impact on estimate qualities. This approach allows us to identify when added complexity improves estimation and when simpler models suffice. Relative to existing literature, Finley et al. (2011) considered spatial effects but did not include county-specific terms, while Pfeiffermann et al. (2008) and Chandra and Sud (2012) did not incorporate spatial dependencies.

To evaluate the nine estimators introduced in Section 2, we conduct a simulation study following the methodology of White et al. (2024a), as described in Section 2.7. Section 3 presents the simulation results and applies the estimators to FIA data, using cross-validation to assess unit-level model performance. Finally, Section 4 summarizes our findings, discusses their implications, and outlines directions for future research.

2 Methods

2.1 Data

The motivating data are from the USDA Forest Service FIA program and comprise inventory plot measurements of live aboveground tree biomass density (Mg/ha). These data were drawn from the most current sampled measurement for each plot in the FIA database downloaded on February 8, 2023 for the states of Washington and Nevada (Burrill et al., 2023). Washington was selected because it has large differences in biomass across counties, ranging from massive biomass densities on the Olympic Peninsula to near zero biomass in counties east of the Cascade Mountain Range. Nevada was selected because it has a fairly unique distribution of forest biomass, where much of the state’s arid environment has little to no biomass which is punctuated with sky islands where there is non-zero forest biomass. Each state has approximately ten years of FIA data, ending in year 2019, that were derived from a panel of plots measured annually across a systematic sample of hexagons approximately 2,500 hectares in size. Biomass values were from live trees only and include all trees 1.0 inch diameter and greater.

Estimators and simulations, described in Sections 2.3 and 2.7, respectively, were informed using five auxiliary variables: National Land Cover Dataset Analytical Tree Canopy Cover 2016 (hereafter `tcc`); LANDFIRE 2010 Digital Elevation Model (hereafter `elev`); US Geological Survey Terrain Ruggedness Index (hereafter `tri`); PRISM mean annual precipitation, 30yr normals (1991-2020) (hereafter `ppt`); and LANDFIRE 2014 tree/non-tree lifeform mask (hereafter `tnt`) (Daly et al., 2002; Rollins, 2009; Yang et al., 2018; Picotte et al., 2019; U.S. Geological Survey, 2019). The `tcc` variable is a measure of average tree canopy cover in a given pixel, the `elev` variable gives the elevation at a given pixel, the `tri` variable gives the terrain ruggedness at a given pixel, the `ppt` variable is a measure of average precipitation at a given pixel over 30 years, and the `tnt` variable is a binary variable distinguishing between pixels with and without trees. These auxiliary variables were resampled to 90 meter resolu-

tion and available wall-to-wall in both states. At locations with FIA plots these variables are matched with the corresponding plot and then used as predictors in the models’ regression components and to inform simulated population generation.

2.2 Variable Selection

The five auxiliary variables described in Section 2.1 were used at multiple stages of analysis, including the generation of simulated populations for Washington and Nevada, the fitting of model-based estimators on these simulated populations, and the application of these estimators to FIA data.

For simulated population generation, variable selection was informed by domain knowledge about regional biomass drivers. In both Washington and Nevada, `tcc` and `elev` were selected as core predictors due to their expected influence on biomass distribution. In Nevada, we additionally included `tri`, given the ecological relevance of sky islands in structuring biomass presence. In Washington, `ppt` was added to reflect the east–west precipitation gradient across the Cascade Range, which significantly influences biomass patterns. To ensure distinct imputation strategies for different vegetation conditions, we stratified the simulated populations in both states by `tnt`.

For the model-based estimators applied to both simulated and FIA data, we used the same predictor variables within each state to maintain consistency with the corresponding data-generating processes. Initially, the `tnt` variable was excluded from model-based estimators. While this exclusion had little effect in Nevada, omitting `tnt` in Washington led to poor predictive performance in the Bernoulli models. As a result, we included `tnt` as a predictor in all Bernoulli models for Washington.

Table 1 summarizes the use of auxiliary variables across model types and data sources.

Predictor	Gaussian	Bernoulli	Simulated population
tcc	WA, NV	WA, NV	WA, NV
elev	WA, NV	WA, NV	WA, NV
tri	NV	NV	NV
ppt	WA	WA	WA
tnt	none	WA	WA, NV

Table 1: Predictor variables used to inform estimators and for generating simulated populations.

2.3 Model-based estimation

We evaluate nine candidate model-based estimators for estimating average biomass density at the county level across Nevada and Washington. The first estimator employs a frequentist approach using a two-stage regression. The remaining eight adopt a Bayesian framework, incorporating both one-stage and two-stage regression structures. A summary of these estimators is provided in Table 2.

All models are fit at the unit level, with plot-level biomass serving as the response variable. To improve adherence to normality assumptions and to ensure positive support for predicted values, we apply a transformation to the response. While logarithmic transformations are common in such contexts, we found them overly aggressive in this application, especially when accommodating zero biomass values, which resulted in highly skewed transformed distributions. Instead, we apply root-based transformations, selecting state-specific powers to match regional biomass distributions: a fourth-root transformation for Washington and a square-root transformation for Nevada.

Although the models are fit at the unit level, our primary inferential target is the average biomass per hectare at the county level, denoted μ_j , where j indexes counties within each state. In the sections that follow, we describe the candidate unit-level models in detail and outline how each is used to estimate these small area parameters of interest.

Estimator	Description
F ZI CVI	A frequentist two-stage estimator. The first stage model is a generalized linear mixed model with a county-varying intercept, and the second stage model is a linear mixed model with a county-varying intercept.
B CVI	A Bayesian single-stage estimator based on a linear mixed model with a county-varying intercept.
B CVC	The same as B CVI, but with county-varying coefficients.
B ZI CVI	A Bayesian two-stage estimator. The first stage model is a generalized linear mixed model with a county-varying intercept, and the second stage model is a linear mixed model with a county-varying intercept.
B ZI CVC	The same as B ZI CVI, but with county-varying coefficients.
B ZI CVI CRV	The same as B ZI CVI, but with county-specific residual variances.
B ZI CVC CRV	The same as B ZI CVC, but with county-specific residual variances.
B ZI CVI SVI CRV	The same as B ZI CVI CRV, but with an added spatial random effect, modeled as a Nearest Neighbor Gaussian process (NNGP) on the intercept.
B ZI CVC SVI CRV	The same as B ZI CVC CRV, but with an added spatial random effect, modeled as a NNGP on the intercept.

Table 2: Description of the candidate models considered for estimating county-level forest biomass. Abbreviations are: frequentist (F); Bayesian (B); zero-inflated (ZI); county-varying intercept (CVI); county-varying coefficient (CVC); county-specific residual variance (CRV); space-varying intercept (SVI).

2.4 Models for frequentist two-stage estimation

Here we introduce the models used to develop a frequentist two-stage approach to estimation (F ZI CVI). The resultant estimator and its MSE estimator were introduced by Chandra and Sud (2012) and later applied to forest inventory data by White et al. (2025) with promising results in the state of Nevada. At generic spatial location ℓ the transformed non-zero forest biomass is modeled as

$$y(\ell) = \beta_0 + \tilde{\beta}_0(\ell) + \mathbf{x}(\ell)^\top \boldsymbol{\beta} + \varepsilon(\ell), \quad (1)$$

where β_0 is the intercept, $\tilde{\beta}_0(\ell)$ is the county specific random effect with $\tilde{\beta}_0(\ell) = \tilde{\beta}_{0,j}$ when ℓ is in the j th county and with $\tilde{\beta}_{0,j} \stackrel{\text{iid}}{\sim} \mathcal{N}(0, \sigma_{\tilde{\beta}_0}^2)$, $\mathbf{x}(\ell)$ is a $p \times 1$ vector of predictor variables, $\boldsymbol{\beta}$ is a $p \times 1$ vector of regression coefficients, and $\varepsilon(\ell)$ is a residual error term with $\varepsilon(\ell) \stackrel{\text{iid}}{\sim} \mathcal{N}(0, \tau^2)$.

Biomass presence and absence is modeled using a Bernoulli mixed model with a logit link function defined as

$$\log \left(\frac{p(\ell)}{1 - p(\ell)} \right) = \alpha_0 + \tilde{\alpha}_0(\ell) + \mathbf{v}(\ell)^\top \boldsymbol{\alpha}, \quad (2)$$

where $p(\ell)$ denotes the probability of non-zero response value at location ℓ , α_0 is the intercept, $\tilde{\alpha}_0(\ell)$ is the county specific random effect with $\tilde{\alpha}_0(\ell) = \tilde{\alpha}_{0,j}$ when ℓ is in the j th county and with $\tilde{\alpha}_{0,j} \stackrel{\text{iid}}{\sim} \mathcal{N}(0, \sigma_{\tilde{\alpha}_0}^2)$, $\mathbf{v}(\ell)$ is a $q \times 1$ vector of predictor variables, $\boldsymbol{\alpha}$ is a $q \times 1$ vector of regression coefficients.

2.5 Models for Bayesian estimation

Here we consider a class of hierarchical Bayesian models. These models are primarily two-stage models similar to the frequentest two-stage model developed in Section 2.4. For comparison, we also include some simpler, single-stage, models that do not explicitly accommodate excess zero values in the response.

The two-stage hierarchical model used in Finley et al. (2011) and adopted here is

$$\begin{aligned} y(\ell) \mid \text{parameters} &\sim \mathcal{N} \left(z(\ell)m(\ell), z(\ell)\tau_1^2 + (1 - z(\ell))\tau_2^2 \right), \\ z(\ell) \mid \text{parameters} &\sim \mathcal{BER} (p(\ell)). \end{aligned} \quad (3)$$

The first level of hierarchy is the model for $z(\ell)$. In our case, we only consider two options for estimation of $z(\ell)$: first, setting $z(\ell)$ to 1; and second, using a linear mixed model with logit link function. In the second case, for simplicity, we only use one model for estimation of $z(\ell)$ across all Bayesian estimators. Here, a realization of $z(\ell)$ indicates whether or not the location ℓ is predicted to have biomass (1) or not (0). Then, we pass the realization

of $z(\ell)$ into the second level of hierarchy where it determines the expression of the mean $m(\ell)$ and the associated variance term. In the subsequent development of models, $m(\ell)$ is a given linear mixed model with county-varying intercept (CVI), county-varying coefficient (CVC), or space-varying intercept (SVI) components (Table 2), resulting in four different model forms for $m(\ell)$ that we implement and compare. The residual variance is estimated through a parameter τ_1^2 when $z(\ell)$ is 1, and set to a small value via a constant, τ_2^2 , when $z(\ell)$ is 0 (see Finley et al., 2011, Section 3 for details). For some candidate models we allow for county-specific residual variance (CRV) terms via county-specific τ_1^2 s (Table 2).

We now turn to the particular models that use the hierarchical structure given by Eq. (3). The simplest model we consider is the county-varying intercept (B CVI) model, which is the Bayesian equivalent to Eq. (1) and is defined as

$$y(\ell) = \beta_0 + \tilde{\beta}_0(\ell) + \mathbf{x}(\ell)^\top \boldsymbol{\beta} + \varepsilon(\ell), \quad (4)$$

with parameter and hyperparameter distributions defined as follows, $\beta_0 \sim \mathcal{N}(0, \sigma_{\beta_0}^2)$, $\tilde{\beta}_0(\ell)$ is the county specific random effect, i.e., $\tilde{\beta}_0(\ell) = \tilde{\beta}_{0,j}$ and $\tilde{\beta}_0(\ell) \stackrel{\text{iid}}{\sim} \mathcal{N}(0, \sigma_{\tilde{\beta}_0}^2)$ when ℓ is in the j th county, $\boldsymbol{\beta} \sim \mathcal{N}(\mathbf{0}, \sigma_{\boldsymbol{\beta}}^2 \mathbf{I})$ with \mathbf{I} being the p -dimensional identity matrix, and $\varepsilon(\ell) \stackrel{\text{iid}}{\sim} \mathcal{N}(0, \tau^2)$, $\sigma_{\tilde{\beta}_0}^2 \sim \mathcal{IG}(a_{\sigma_{\tilde{\beta}_0}^2}, b_{\sigma_{\tilde{\beta}_0}^2})$, and $\tau^2 \sim \mathcal{IG}(a_{\tau^2}, b_{\tau^2})$. All hyperparameters were set to induce non-informative prior distributions.

Next, we consider the county-varying coefficient (B CVC) model that allows regression coefficients to vary by county. This model is defined as

$$y(\ell) = \beta_0 + \tilde{\beta}_0(\ell) + \mathbf{x}(\ell)^\top (\boldsymbol{\beta} + \tilde{\boldsymbol{\beta}}(\ell)) + \varepsilon(\ell), \quad (5)$$

where $\tilde{\boldsymbol{\beta}}(\ell) = (\tilde{\beta}_{1,j}, \tilde{\beta}_{2,j}, \dots, \tilde{\beta}_{p,j})^\top$ with $\tilde{\beta}_{k,j} \stackrel{\text{iid}}{\sim} \mathcal{N}(0, \sigma_{\tilde{\beta}_{k,j}}^2)$ and $\sigma_{\tilde{\beta}_{k,j}}^2 \sim \mathcal{IG}(a_{\sigma_{\tilde{\beta}_{k,j}}^2}, b_{\sigma_{\tilde{\beta}_{k,j}}^2})$ for $k = 1, 2, \dots, p$ when ℓ is in the j th county.

The B CVI and B CVC models defined above are used in our analyses both as a single-stage model (by setting $z(\ell) = 1$ in the hierarchical model) and in the two-stage setting.

We are most interested in these simpler, single-stage, models for comparison with two-stage models as laid out in Table 2.

Turning now to the two-stage models. Each two-stage model introduced in this section uses the same first stage model; however, the framework we defined in Eq. (3) lends itself to a variety of different second stage models. We consider a range of second stage models.

The first stage model used for all two-stage models is the Bayesian equivalent to Eq. (2), a generalized linear mixed model with Bernoulli response and a county-varying intercept defined as

$$\log \left(\frac{p(\ell)}{1 - p(\ell)} \right) = \alpha_0 + \tilde{\alpha}_0(\ell) + \mathbf{v}(\ell)^\top \boldsymbol{\alpha}, \quad (6)$$

where $p(\ell)$ denotes the probability of non-zero response, and parameter and hyperparameter distributions are defined as follows, $\alpha_0 \sim \mathcal{N}(0, \sigma_{\alpha_0}^2)$, $\tilde{\alpha}_0(\ell)$ is the county specific random effect, i.e., $\tilde{\alpha}_0(\ell) = \tilde{\alpha}_{0,j}$ and $\tilde{\alpha}_0(\ell) \stackrel{\text{iid}}{\sim} \mathcal{N}(0, \sigma_{\tilde{\alpha}_0}^2)$ when ℓ is in the j th county, $\boldsymbol{\alpha} \sim \mathcal{N}(\mathbf{0}, \sigma_{\boldsymbol{\alpha}}^2 \mathbf{I})$, and $\sigma_{\tilde{\alpha}_0}^2 \sim \mathcal{IG}(a_{\sigma_{\tilde{\alpha}_0}^2}, b_{\sigma_{\tilde{\alpha}_0}^2})$. All hyperparameters were set to induce non-informative prior distributions.

Now, we can combine Eq. (6) with Eq. (4) and specify the first two-stage hierarchical model (B ZI CVI) as

$$y(\ell) = z(\ell) \left(\beta_0 + \tilde{\beta}_0(\ell) + \mathbf{x}(\ell)^\top \boldsymbol{\beta} \right) + z(\ell)\varepsilon_1(\ell) + (1 - z(\ell))\varepsilon_2(\ell), \quad (7)$$

where $\varepsilon_1(\ell) \stackrel{\text{iid}}{\sim} \mathcal{N}(0, \tau_1^2)$ and $\varepsilon_2(\ell) \stackrel{\text{iid}}{\sim} \mathcal{N}(0, \tau_2^2)$ with $\tau_1^2 \sim \mathcal{IG}(a_{\tau_1^2}, b_{\tau_1^2})$ and $\tau_2^2 = 0.00001$.

The hierarchical model specified in Eq. (7) is analogous to the frequentist two-stage model specified in Section 2.4. Notably, this hierarchical structure combines the Bernoulli model with the B CVI model to produce estimates that account for zero inflation.

We next extend Eq. (7) to include county-varying coefficients (B ZI CVC) defined as

$$y(\ell) = z(\ell) \left(\beta_0 + \tilde{\beta}_0(\ell) + \mathbf{x}(\ell)^\top \left(\boldsymbol{\beta} + \tilde{\boldsymbol{\beta}}(\ell) \right) \right) + z(\ell)\varepsilon_1(\ell) + (1 - z(\ell))\varepsilon_2(\ell). \quad (8)$$

In practice, it is common for residual variance to increase with increasing biomass, i.e., heteroscedasticity. Given disparity in forest density at the county-level, we might expect residual variance to vary across counties. For example, western counties in Washington have much more forest biomass than counties in eastern Washington, and if this disparity in biomass is not entirely captured by the predictors and random effects, then we would expect quite different residual variances. A county-specific residual variance term can help accommodate heteroscedasticity and improve county-level estimates; hence, we extend the B ZI CVI Eq. (7) and B ZI CVC Eq. (8) models with county-specific residual variance parameters. Specifically, the zero-inflated county-varying intercept model with county-specific residual variance (B ZI CVI CRV) and the corresponding county-varying coefficient model (B ZI CVC CRV) are defined analogous to Eq. (7) and Eq. (8) but with $\varepsilon_1(\ell) \stackrel{\text{iid}}{\sim} \mathcal{N}(0, \tau_{1,j}^2)$ with $\tau_{1,j}^2 \sim \mathcal{IG}(a_{\tau_1^2}, b_{\tau_1^2})$ when ℓ is in the j th county.

In addition to county scale differences in mean biomass and predictor variables' relationships with biomass, captured through county-varying intercepts and county-varying coefficients, respectively, we might expect to see smoothly-varying spatially structured changes in mean biomass caused by disturbance history, climate impacts, species composition, or any spatially dependent factors not captured by predictors variables. Such spatial changes in mean biomass can be accommodated via a space-varying intercept random effect. The models below extend the B ZI CVI CRV and B ZI CVC CRV models to include such a space-varying intercept. Specifically, the B ZI CVI SVI CRV model is defined as

$$y(\ell) = z(\ell) \left(\beta_0 + \tilde{\beta}_0(\ell) + \mathbf{x}(\ell)^\top \boldsymbol{\beta} + w(\ell) \right) + z(\ell)\varepsilon_1(\ell) + (1 - z(\ell))\varepsilon_2(\ell), \quad (9)$$

where $w(\ell)$ is a spatial random effect that adjusts the intercept based on residual spatial dependence. Here we estimate $w(\ell)$ using a Gaussian Process approximation called the Nearest Neighbor Gaussian Process (NNGP; Datta et al. 2016; Finley et al. 2019) that provides substantial improvements in run time, with negligible differences in inference and predic-

tion, compared to a model that uses a full Gaussian Process. In brief, for this specification, the vector of random effects collected over n locations $\mathbf{w} = (w(\ell_1), w(\ell_2), \dots, w(\ell_n))^\top$ is distributed multivariate normal with mean zero and covariance matrix that captures the spatial dependence among random effects, i.e., $\mathbf{w} \sim \mathcal{MVN}(\mathbf{0}, \sigma_w^2 \mathbf{R}(\phi))$, where σ_w^2 is the spatial variance and $\mathbf{R}(\phi)$ is the NNGP-derived correlation matrix that depends on a spatial correlation function, which in our case is exponential, and decay parameter ϕ used to estimate the strength of correlation between any two locations. As with other variance parameters, we assume $\sigma_w^2 \sim \mathcal{IG}(a_{\sigma_w^2}, b_{\sigma_w^2})$ with hyperparameters set to induce a non-informative prior distribution. The spatial decay parameter is assumed to follow a uniform distribution with broad, non-informative, spatial support.

The last candidate model ZI CVC SVI CRV extends B ZI CVI SVI CRV Eq. (9) to include county-varying coefficients.

2.6 Model implementation and comparison

2.6.1 Frequentist two-stage estimator

Model parameters for the two-stage frequentist model (F ZI CVI) described in Section 2.4 were estimated using restricted maximum likelihood via the R (R Core Team, 2024) `saeczi` package (Yamamoto et al., 2025) which implements methods presented by Chandra and Sud (2012).

As described in Section 1, to generate estimates for a small area of interest, we predict biomass and probability of non-zero biomass using Eq. (1) and Eq. (2) respectively, over a fine grid of prediction locations. For generic prediction location ℓ^* these predictions are

$$y(\ell^*) = \hat{\beta}_0 + \hat{\beta}_0(\ell^*) + \mathbf{x}(\ell^*)^\top \hat{\boldsymbol{\beta}}, \quad \text{and} \quad p(\ell^*) = \frac{\exp\left(\hat{\alpha}_0 + \hat{\alpha}_0(\ell^*) + \mathbf{v}(\ell^*)^\top \hat{\boldsymbol{\alpha}}\right)}{1 + \exp\left(\hat{\alpha}_0 + \hat{\alpha}_0(\ell^*) + \mathbf{v}(\ell^*)^\top \hat{\boldsymbol{\alpha}}\right)}, \quad (10)$$

where the $\hat{\cdot}$ indicates each parameter's maximum likelihood point estimate. The estimate

for μ_j is then the average product of these predictions over the grid of prediction locations

$$\hat{\mu}_j = \frac{1}{n_j^*} \sum_{\ell \in U_j} g^{-1}(y(\ell^*)) p(\ell^*), \quad (11)$$

where $g^{-1}(\cdot)$ is the inverse of the transformation function used when fitting the model, allowing us to revert back to biomass scale, and U_j is the set of n^* prediction locations within the j th county. This estimator's MSE estimator comes from a parametric bootstrap introduced in Chandra and Sud (2012) and discussed and explored in White et al. (2025).

2.6.2 Bayesian estimators

Parameter inference for Bayesian models described in Section 2.5 was based on MCMC samples from posterior distributions. Gibbs and Metropolis Hastings algorithms were implemented in C++ to efficiently sample from parameter posterior distributions. Code, additional information about the sampling algorithms, and example analyses using simulated data are given in Finley (2025) and a list of prior distributions and hyperparameter values is given in Appendix A. Posterior inference is based on $M=3,000$ post-convergence and thinned samples from three MCMC chains, i.e., 1,000 from each chain. We use convergence diagnostics and thinning rules outlined in Gelman et al. (2013).

Inference about biomass at prediction locations and subsequent county-level estimates for μ_j are based on posterior predictive distribution samples. All single- and two-stage models follow the same approach for predictive inference, which is based on composition sampling from each model's posterior predictive distribution. For example, using the B ZI CVI SVI CRV Eq. (9) model, for generic prediction location ℓ^* we generate M post-convergence and thinned samples one-for-one, first plugging in the s th MCMC sample of model parameters into the model's predictive distribution to generate a corresponding posterior predictive distribution sample. Specifically, for $s = 1, 2, \dots, M$ we draw a sample from the posterior

predictive distribution for forest presence/absence

$$z^{(s)}(\ell^*) \sim \mathcal{RBER} \left(\frac{\exp \left(\alpha_0^{(s)} + \tilde{\alpha}_0^{(s)}(\ell^*) + \mathbf{v}(\ell^*)^\top \boldsymbol{\alpha}^{(s)} \right)}{1 + \exp \left(\alpha_0^{(s)} + \tilde{\alpha}_0^{(s)}(\ell^*) + \mathbf{v}(\ell^*)^\top \boldsymbol{\alpha}^{(s)} \right)} \right) \quad (12)$$

then, given $z^{(s)}(\ell^*)$, we draw from the posterior predictive distribution for transformed biomass

$$y^{(s)}(\ell^*) \sim \mathcal{RN} \left(z^{(s)}(\ell^*) \left(\beta_0^{(s)} + \tilde{\beta}_0^{(s)}(\ell^*) + \mathbf{x}(\ell^*)^\top \boldsymbol{\beta}^{(s)} + w^{(s)}(\ell^*) \right), \right. \\ \left. z^{(s)}(\ell^*) \tau_1^{2(s)} + (1 - z^{(s)}(\ell^*)) \tau_2^{2(s)} \right), \quad (13)$$

where \mathcal{RBER} and \mathcal{RN} generate a random draw from a Bernoulli and normal distribution, respectively.

Given M posterior predictive samples from Eq. (13), we can draw corresponding samples for county-level means. Specifically, samples from the j th county's posterior predictive distribution are drawn one-for-one from

$$\mu_j^{(s)} = \frac{1}{n_j^*} \sum_{\ell \in U_j} g^{-1} \left(y^{(s)}(\ell^*) \right), \quad (14)$$

for $s = 1, 2, \dots, M$.

For subsequent comparison and mapping, we calculate the mean and credible intervals using samples from the desired posterior predictive distribution. For example, the Bayesian equivalent to Eq. (11) is computed $\hat{\mu}_j = \sum_{s=1}^M \mu_j^{(s)} / M$.

2.6.3 Metrics for comparison

We now discuss the metrics used for evaluating estimators in Section 3.1 and unit-level predictions via cross-validation in Section 3.2. Since we evaluate both unit-level predictions and areal estimates with these metrics, we use generic θ and $\hat{\theta}$ to denote a parameter of

interest and an estimate of that parameter of interest, respectively.

First the root mean square error (RMSE) is as follows,

$$\text{RMSE}(\hat{\theta}) = \sqrt{\frac{1}{m} \sum_{i=1}^m (\hat{\theta}_i - \theta)^2}, \quad (15)$$

where m is the number of estimates produced for the given parameter of interest. We evaluate this metric empirically across simulation repetitions and hold-out sets for areal estimates and unit-level predictions, respectively. Next, the bias is as follows

$$\text{Bias}(\hat{\theta}) = \mathbb{E}(\hat{\theta}) - \theta, \quad (16)$$

where $\mathbb{E}(\hat{\theta})$ is computed empirically across the design-based samples. We use the bias metric to evaluate the bias of estimates, estimates of the RMSE, and unit-level predictions in subsequent sections. Similar to the RMSE, the bias metric is evaluated empirically. Finally, the indicator of coverage for a given uncertainty interval C is

$$\mathbb{1}_C(\hat{\theta}) = \begin{cases} 1, & \text{if } \hat{\theta} \in C, \\ 0, & \text{if } \hat{\theta} \notin C. \end{cases} \quad (17)$$

2.7 Simulation

We conducted a simulation study to evaluate the performance of the estimators introduced in Section 2.3. Simulation studies are especially valuable in SAE assessment, as they allow for comparisons against known true parameter values, thereby providing direct insight into estimator performance. To ensure a fair and realistic evaluation, we followed the methodology proposed by White et al. (2024a).

Briefly, this approach uses a k -nearest neighbors (k NN) algorithm applied to auxiliary data, with neighbors weighted by bootstrap inclusion probabilities, to impute forest inventory

attributes at each population unit. The complete algorithm for generating a population for a given state is presented in Algorithm 1 of White et al. (2024a).

Simulated populations were generated separately for Washington and Nevada. As described in Section 2.1, auxiliary variables used in the k NN matching included `tcc`, `elev`, and `ppt` in Washington, and `tcc`, `elev`, and `tri` in Nevada. In both states, `tnt` was used as a stratification variable to distinguish between treed and non-treed areas. Prior to matching, all auxiliary variables were centered (mean zero) and scaled (unit variance) to prevent differences in variable magnitude from disproportionately influencing the k NN search. The population generation process was implemented using the `kbaabb` R package (White et al., 2024b).

Following population generation, we drew design-based samples to assess estimator performance. For each simulation replicate, we selected a simple random sample within each county, matching the number of FIA plots observed in that county. This ensured that both county-level and overall sample sizes remained consistent with the original FIA data.

3 Results

This section presents the results of the simulation study and the FIA data application, discussed in Sections 3.1 and 3.2, respectively. In Section 3.1, we assess estimator performance using the metrics defined in Section 2.6.3. Section 3.2 provides county-level biomass estimates and evaluates estimator performance based on cross-validation.

3.1 Simulation Study

We evaluated the nine estimators introduced in Section 2 using repeated samples drawn from the simulated populations described in Section 2.7. Model fitting was performed separately for Nevada and Washington to reflect state-specific differences in data-generating processes. Estimator performance was assessed using the metrics defined in Section 2.6.3. Notably,

performance varied between states, likely due to substantial ecological differences: Nevada’s forests are largely confined to high-elevation sky islands, whereas Washington’s forests are primarily located west of the Cascade Range, where precipitation and productivity are substantially higher.

Figure 1 presents the estimator performance metrics for Nevada. Each point in the figure represents a county–metric–estimator combination. In Figure 1a, we observe that single-stage estimators tend to exhibit the greatest empirical bias. Additionally, estimators that do not account for county-specific variances generally perform worse in terms of bias than those that do. The least biased estimators are the B ZI CVI CRV and B ZI CVI SVI CRV, which yield nearly identical results. Comparisons between the CVC and CVI model structures reveal that, in Nevada, the inclusion of CVC terms typically increases empirical bias once CRV and/or SVI terms are added.

These trends are even more pronounced in Figure 1b, which displays empirical root mean squared error (RMSE). Models with CVC terms consistently show higher RMSE values than their CVI-based counterparts. Among the CVI-based two-stage estimators, RMSE performance is comparable across models. Conversely, models without CVI terms also perform similarly to one another but lag behind the CVI-based estimators.

Figure 1c shows the empirical bias in RMSE estimation, which reflects whether an estimator under- or over-estimates its own uncertainty. The B CVI and B CVC models significantly underestimate their RMSE, likely due to poor model specification. Somewhat unexpectedly, the B ZI CVI estimator also shows RMSE underestimation, despite accounting for zero-inflation. The F ZI CVI model estimates its RMSE reasonably well but displays greater variability compared to the B ZI models that include CRV and/or SVI effects, which generally yield accurate RMSE estimates but occasionally produce negative outliers.

Lastly, Figure 1d illustrates empirical 95% uncertainty interval coverage. The B CVI and B CVC estimators again perform poorly, exhibiting undercoverage across many counties. While the F ZI CVI estimator performs better than its Bayesian counterpart in this regard,

both show some counties with notably low coverage. The remaining estimators—including those incorporating zero-inflation, CRV, and SVI components—demonstrate strong and consistent coverage performance, with the B ZI CVI SVI CRV estimator yielding median coverage closest to the desired value, 0.95.

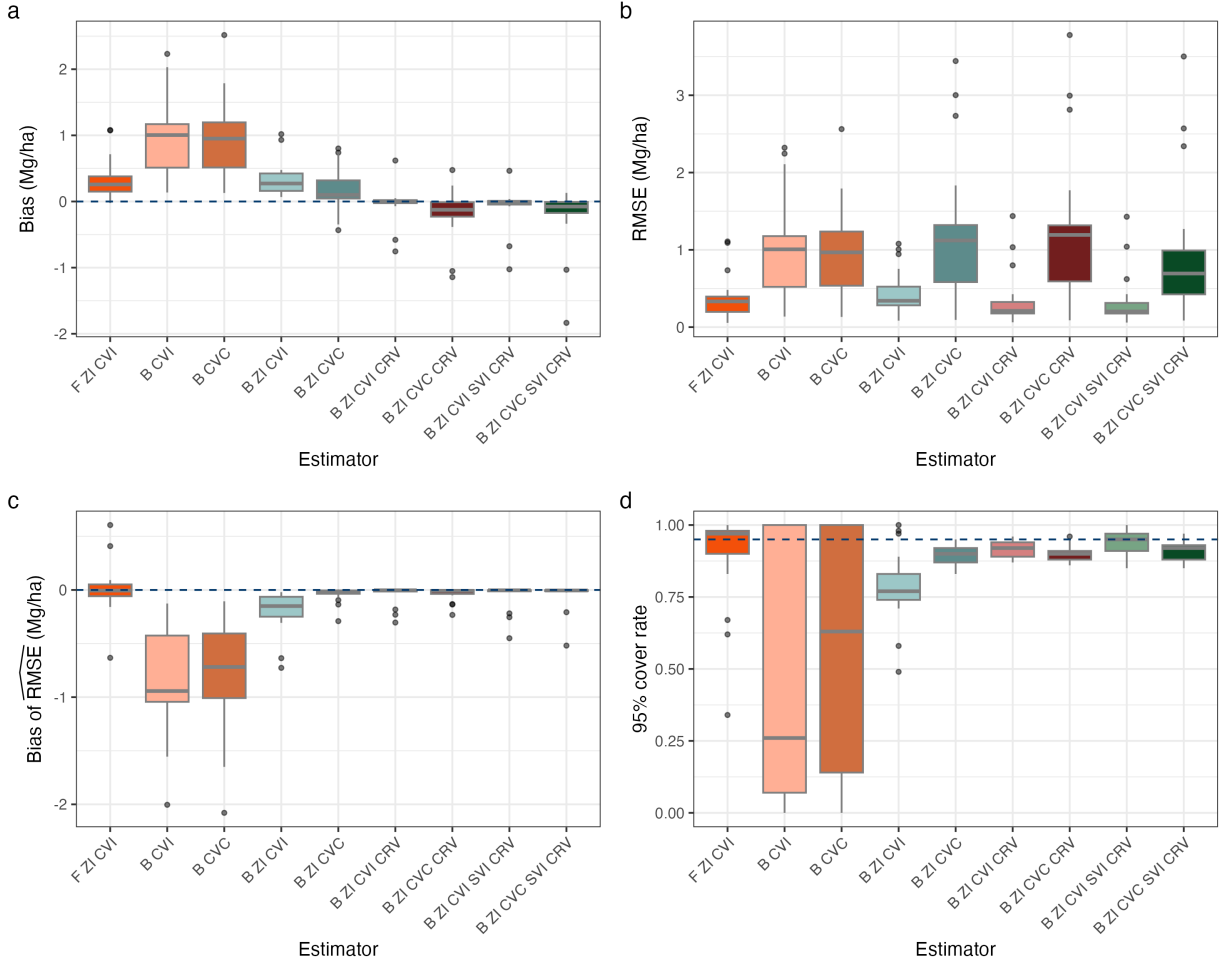


Figure 1: Estimator performance metrics in Nevada. The x-axis and fill corresponds to estimator and the y-axis corresponds to the value of the performance metric. Each point represents the performance metric in a given county for a particular estimator. (a) shows the estimator’s empirical bias, (b) shows the estimator’s empirical root mean square error (RMSE), (c) shows the empirical bias of the RMSE estimator, and (d) shows the estimator’s empirical 95% uncertainty interval coverage rate. Abbreviations are: root mean square error (RMSE); frequentist (F); zero-inflated (ZI); county-varying intercept (CVI); Bayesian (B); county-varying coefficient (CVC); county-specific residual variance (CRV); space-varying intercept (SVI).

Figure 2 presents the estimator performance metrics for Washington, where each point

represents a county–metric–estimator combination. Figure 2a displays empirical bias. The F ZI CVI estimator exhibits the highest bias among all estimators—substantially more than its Bayesian counterpart, B ZI CVI. Although the two estimators are structurally similar, this discrepancy is likely attributable to differences in how each handles the back-transformation of the response variable. The frequentist estimator applies the back-transformation directly to the predicted mean, whereas Bayesian estimators apply it to each sample from the posterior predictive distribution, which can yield more accurate and robust estimates, especially in non-linear settings.

The B CVI and B CVC estimators also exhibit relatively high bias compared to the two-stage Bayesian models, all of which show comparable and generally lower bias. Interestingly, the B ZI CVC CRV and B ZI CVC SVI CRV estimators display slightly higher bias than their CVI-based counterparts. As shown in Figure 2b, these same estimators also have higher empirical RMSE. The B ZI CVI CRV and B ZI CVI SVI CRV estimators yield the lowest RMSE values overall, while the F ZI CVI estimator exhibits the highest RMSE. Other two-stage Bayesian estimators have similar RMSE values, with single-stage estimators performing slightly worse.

Figure 2c shows the empirical bias in RMSE estimation. The F ZI CVI and B CVI estimators perform poorly when estimating their own variability, whereas most other estimators—particularly those incorporating CRV terms—demonstrate minimal bias and precise estimation of their own variability. This suggests that accounting for county random variation improves the accuracy of uncertainty estimation.

Finally, Figure 2d presents empirical 95% uncertainty interval coverage. The B CVI and B CVC estimators perform poorly in this regard, with consistently low coverage rates across counties. In contrast, the remaining estimators—all two-stage models—achieve more reliable coverage. Notably, those incorporating both CVC effects and CRV terms, such as B ZI CVC SVI CRV, exhibit the best coverage performance.

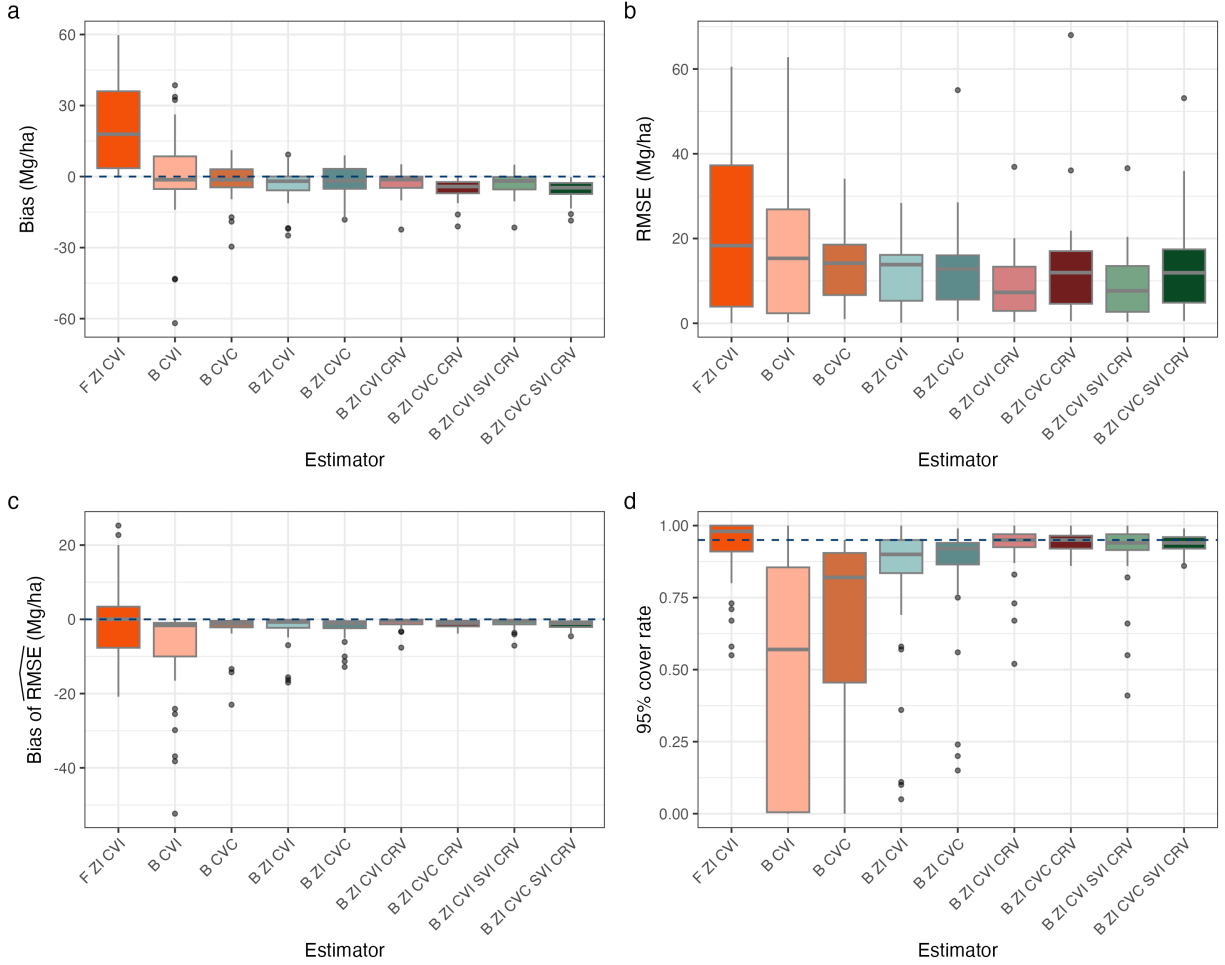


Figure 2: Estimator performance metrics in Washington. The x-axis and fill corresponds to estimator and the y-axis corresponds to the value of the performance metric. Each point represents the performance metric in a given county for a particular estimator. (a) shows the estimator’s bias, (b) shows the estimator’s root mean square error (RMSE), (c) shows the bias of the RMSE estimator, and (d) shows the estimator’s 95% uncertainty interval coverage rate. Abbreviations are: root mean square error (RMSE); frequentist (F); zero-inflated (ZI); county-varying intercept (CVI); Bayesian (B); county-varying coefficient (CVC); county-specific residual variance (CRV); space-varying intercept (SVI).

Stepping back from the specific results presented in Figures 1 and 2, several broader insights emerge regarding the estimators and the simulation study design. One notable finding is the minimal performance difference between estimators that include a spatially varying intercept (SVI) and their non-spatial counterparts. This observation should not be interpreted as evidence against the utility of spatial effects in modeling forest attributes. On

the contrary, previous studies have demonstrated the substantial benefits of incorporating spatial structure in such settings (Finley et al., 2024). Moreover, the cross-validation results presented in Section 3.2 show that spatial models often yield more accurate predictions when applied to real FIA data.

The lack of benefit from SVI models in the simulation study is likely attributable to the limited spatial structure in the simulated populations. Upon inspection, the populations generated via the k NN-based approach exhibit weak spatial autocorrelation. This suggests that the simulation framework, while useful for certain evaluations, may not be well suited for assessing the potential advantages of spatial models. Future simulation designs could benefit from incorporating spatial smoothing or explicitly modeling spatial dependence during population generation to more accurately reflect the structure observed in real-world forest systems.

Another general finding is the limited utility of models incorporating CVC effects. In many cases—particularly in Nevada—CVC models not only failed to improve estimator performance but also introduced greater bias and RMSE. This may be due to the relative homogeneity of county-level biomass in Nevada, which provides limited justification for allowing predictor effects to vary by county. In contrast, in Washington—where forest types and biomass distributions are more heterogeneous—CVC-based estimators exhibited better 95% uncertainty interval coverage than their constant-coefficient counterparts. However, these gains came at the cost of increased bias and RMSE. These results suggest that CVC effects may be more beneficial in broader applications involving larger spatial domains—such as national-level analyses—or in regions with more diverse ecological conditions, where predictor–response relationships are expected to vary more substantially across space.

3.2 FIA data application

We applied the candidate estimators to FIA plot data collected in Nevada and Washington. We first evaluated performance using 10-fold cross-validation, followed by an examination

of county-level biomass estimates produced by the B ZI CVI SVI CRV estimator, which performed favorably in both the simulation study and cross-validation.

Cross-validation was conducted at the unit level, with unit-level predictions used as a proxy for estimating county-level means. Results are presented in Table 3. For Bayesian estimators, 95% uncertainty interval coverage rates (“Coverage” in Table 3) were computed using quantiles of the posterior predictive distribution of $y(\ell)$. Coverage is not reported for the frequentist estimator, as deriving either closed-form or bootstrap-based prediction intervals at the unit level for the two-stage model is beyond the scope of this study.

The results exhibit patterns similar to those observed in the simulation study (Figures 1 and 2), but with clearer improvements associated with spatial models—particularly in terms of root mean square prediction error (RMSPE) and empirical bias. Across both states, estimators incorporating a county-specific variance term consistently showed favorable bias and coverage rates. In Nevada, estimators accounting for zero-inflation also performed notably well.

These cross-validation results reinforce findings from the simulation study and provide complementary insights into estimator performance under realistic sampling conditions. We further discuss the relative merits of simulation-based and cross-validation-based evaluation strategies in Section 4.

In both Nevada and Washington, the B ZI CVI SVI CRV estimator performed consistently well across all metrics evaluated in the simulation study and cross-validation. As a result, we selected this estimator to produce pixel-level predictions and county-level biomass estimates in each state.

Figure 3a and 3b display pixel-level estimates of biomass probability, while Figure 3c and 3d show pixel-level estimates of biomass (Mg/ha) in Washington and Nevada, respectively. Although pixel-level predictions are not the primary focus of this study, such maps can be valuable for forest management at finer spatial scales, such as the stand level. Within the

State	Metric	F ZI CVI	B CVI	B CVC	B ZI CVI	B ZI CVC	B ZI CVI CRV
WA	RMSPE	107.05	113.90	111.48	106.87	104.78	104.03
WA	Bias	18.10	22.49	19.75	17.52	15.49	-1.63
WA	Coverage	NA	42.95	49.10	65.00	69.41	96.77
NV	RMSPE	7.79	8.17	8.27	7.79	9.30	7.82
NV	Bias	0.35	0.85	0.88	0.33	-0.24	0.00
NV	Coverage	NA	49.95	68.79	91.57	95.41	97.85
State	Metric	B ZI CVC CRV		B ZI CVI SVI CRV		B ZI CVC SVI CRV	
WA	RMSPE	103.17		98.62		99.15	
WA	Bias	-3.21		-2.15		-3.71	
WA	Coverage	96.59		96.71		96.68	
NV	RMSPE	8.90		7.77		7.73	
NV	Bias	-0.35		0.00		-0.02	
NV	Coverage	97.99		98.04		97.92	

Table 3: Results for each estimator and state from the unit-level cross-validation. Results include empirical measures of root mean square prediction error, bias, and 95% uncertainty interval coverage rate. Abbreviations are: Washington (WA); Nevada (NV); root mean square prediction error (RMSPE); frequentist (F); zero-inflated (ZI); county-varying intercept (CVI); Bayesian (B); county-varying coefficient (CVC); county-specific residual variance (CRV); space-varying intercept (SVI).

Bayesian framework, pixel-level predictions are accompanied by corresponding uncertainty estimates, enabling flexible spatial summarization. While we report aggregated estimates at the county level for this analysis, the same framework allows for the generation of estimates and associated uncertainties for any user-defined spatial unit (e.g., ecoregions, watersheds, fire perimeters, or management units) using any of the Bayesian estimators considered.

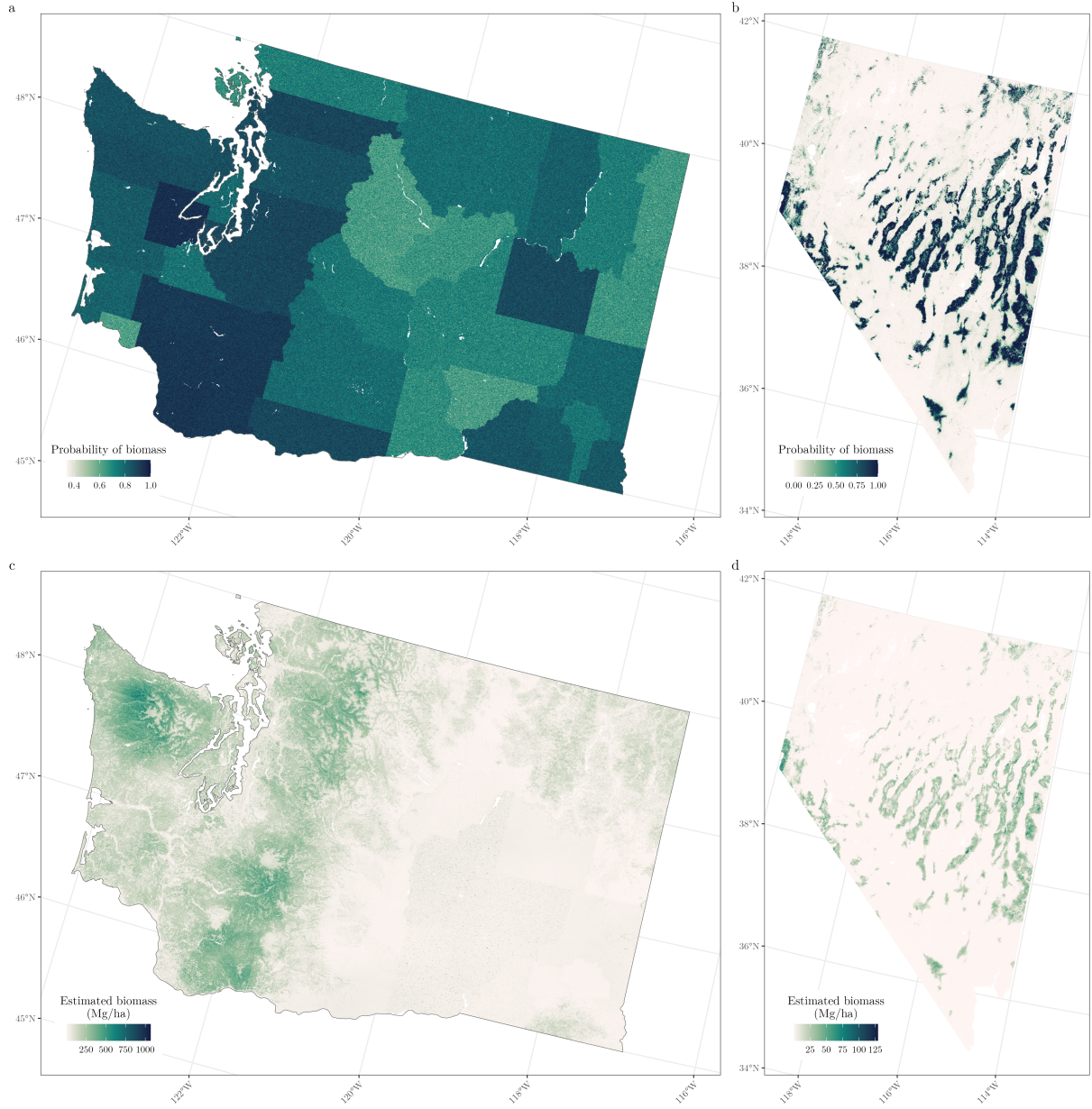


Figure 3: Pixel-level estimates of biomass probability (a, b) and estimated biomass (c, d) in Washington (a, c) and Nevada (b, d). Pixel-level estimates of biomass probability are produced from the Bayesian model with Bernoulli response and county varying intercept. Pixel-level estimates of biomass are produced from the Bayesian zero-inflated model with county varying intercept with space varying intercept and county specific variances.

Figure 4 presents the resulting county-level biomass estimates for both states, generated using the B ZI CVI SVI CRV estimator. These county-level estimates represent the primary inferential target for SAE in this study. As expected, the results for Washington show

a pronounced gradient in biomass across the Cascade Range, while biomass estimates in Nevada appear relatively homogeneous across counties.

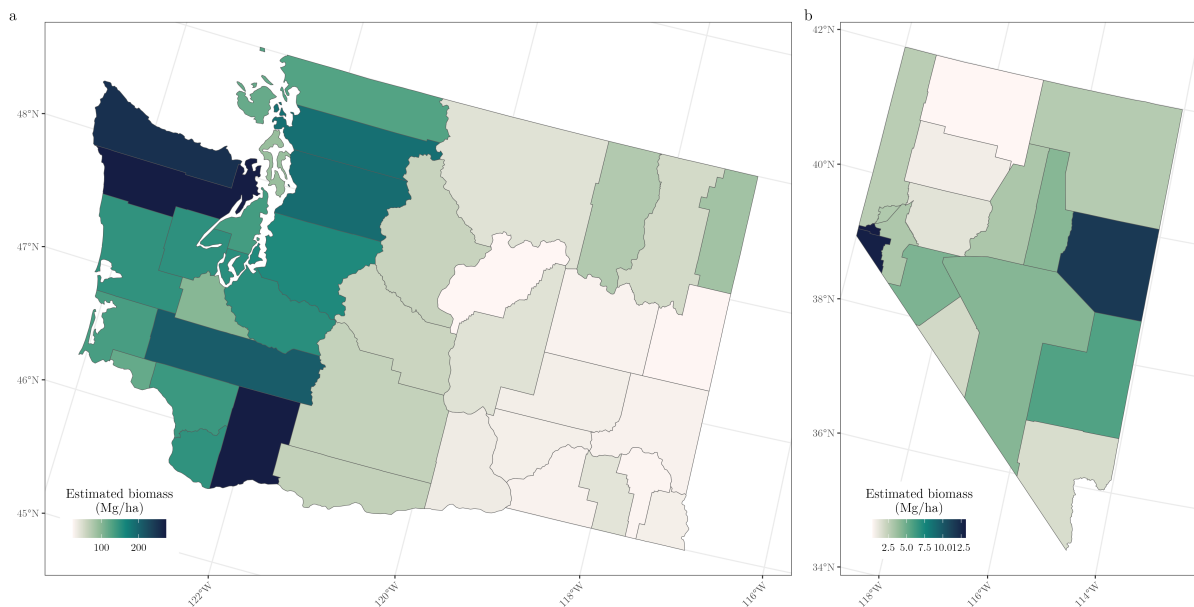


Figure 4: County-level estimates of average biomass (Mg/ha) in Washington (a) and Nevada (b). Estimates are produced from the Bayesian zero-inflated model with county varying intercept with space varying intercept and county specific variances.

4 Discussion and Conclusion

We implemented and compared nine model-based estimators—spanning both frequentist and Bayesian frameworks—for estimating biomass at the county level in Nevada and Washington. The Bayesian estimators offered flexibility in model specification, allowing the inclusion of CVIs, CVCs, CRVs, and SVIs. To evaluate these estimators, we used two complementary strategies: a simulation study based on design-based sampling from a bootstrap-weighted k NN-generated population, and unit-level cross-validation using FIA data. Overall, the results indicate that estimators incorporating two-stage zero-inflation modeling, CRVs, and SVIs performed best.

One notable finding emerged from a comparison between the F ZI CVI and B ZI CVI estimators in Washington. While these estimators yielded similar results in Nevada, they

diverged considerably in Washington. Given their comparable model forms, such divergence is initially surprising. However, the discrepancy stems from differences in how the response variable is back-transformed in the two paradigms. In the frequentist setting, predictions are back-transformed using the maximum likelihood point estimate $\hat{y}(\ell)$, whereas the Bayesian approach applies the back-transformation to each draw from the posterior predictive distribution at location ℓ . In Washington—where the biomass distribution is heavily skewed—the frequentist approach fails to capture the non-symmetric distributional shape, resulting in biased predictions. The Bayesian approach, by contrast, preserves the skewness and produces more realistic estimates.

Evaluating estimators for SAE is inherently challenging due to small sample sizes within target areas and the absence of true parameter values at those granular scales. To address this, we adopted two evaluation frameworks, each with tradeoffs. The first—simulation-based evaluation—enables empirical comparison against known true values through repeated sampling from a synthetic population. This method is valid provided two conditions are met: (1) the simulated population is not overly similar to the estimation models, and (2) it sufficiently resembles the real-world population. We addressed (1) by adopting the bootstrap-weighted k NN generation method proposed by White et al. (2024a). However, condition (2) was only partially met. Specifically, the generated population exhibited limited spatial autocorrelation—unlike what is typically observed in real forest systems. As a result, estimators incorporating SVIs did not demonstrate their full potential in the simulation setting.

The cross-validation analysis offered a complementary perspective, free from assumptions about the population generation process. While it does not directly assess small area means, it allows for meaningful evaluation of unit-level prediction accuracy. In our case, the cross-validation results aligned well with those from the simulation study but also highlighted the added value of spatial models—particularly those including SVIs and CRVs—under realistic conditions. A limitation of this approach is that it is only applicable to unit-level models and necessitates accepting unit-level predictions as a proxy for small area estimates.

Our findings offer practical guidance for estimating biomass—or other continuous, zero-inflated forest attributes—across heterogeneous landscapes. In the context of a changing climate and increasing disturbance regimes such as wildfires, the need for accurate, small area estimates of forest structure is more critical than ever. One limitation of this study is the lack of spatial structure in the simulated populations, which limited the utility of simulations for evaluating spatial estimators. To address this, future work will incorporate spatial dependence into population generation using non-parametric spatial smoothing techniques.

Beyond methodological refinement, future research will focus on extending these estimators to additional spatial units of ecological interest—such as recently burned areas, forest stands, or watersheds—and to temporal applications for monitoring biomass change over time. These directions will enhance the utility of model-based SAE methods for forest inventory and broader environmental monitoring.

Author statements

Competing interests statement

JKY is employed by RedCastle Resources, Inc. GWW is part-time employed by RedCastle Resources, Inc. The remaining authors declare that the research was conducted in the absence of any commercial or financial relationships that could be construed as a potential conflict of interest.

Funding statement

This work was supported by the: US Forest Service (USFS) Forest Inventory and Analysis Program; USFS Region 9, Forest Health Protection; Michigan State University AgBioResearch; National Science Foundation DEB-2213565 and DEB-1946007; National Aeronautics and Space Administration CMS Hayes-2023. The findings and conclusions in this publication are those of the authors and should not be construed to represent any official US Department

of Agriculture or US Government determination or policy.

Data availability statement

The data include confidential plot data, which can not be shared publicly. FIA data can be accessed through the FIA DataMart (<https://apps.fs.usda.gov/fia/datamart/datamart.html>). Requests for data used here or other requests including confidential data should be directed to FIA's Spatial Data Services (<https://www.fs.usda.gov/research/programs/fia/sds>).

References

- Battese, G. E., Harter, R. M., and Fuller, W. A. (1988). An error-components model for prediction of county crop areas using survey and satellite data. *Journal of the American Statistical Association*, 83(401):28–36.
- Burrill, E., Christensen, G., Conkling, B., DiTommaso, A., Lepine, L., Perry, C., Pugh, S., Turner, J., Walker, D., and Williams, M. (2023). Forest inventory and analysis database: Database description and user guide for phase 2 (version: 9.1).
- Cao, Q., Dettmann, G. T., Radtke, P. J., Coulston, J. W., Derwin, J., Thomas, V. A., Burkhart, H. E., and Wynne, R. H. (2022). Increased precision in county-level volume estimates in the united states national forest inventory with area-level small area estimation. *Frontiers in Forests and Global Change*, 5:769917.
- Chandra, H. and Sud, U. C. (2012). Small area estimation for zero-inflated data. *Communications in Statistics - Simulation and Computation*, 41:632 – 643.
- Daly, C., Gibson, W. P., Taylor, G. H., Johnson, G. L., and Pasteris, P. (2002). A knowledge-based approach to the statistical mapping of climate. *Climate Research*, 22(2):99–113.
- Datta, A., Banerjee, S., Finley, A. O., and Gelfand, A. E. (2016). Hierarchical nearest-neighbor Gaussian process models for large geostatistical datasets. *Journal of the American Statistical Association*, 111(514):800–812.
- Fay, R. E. I. and Herriot, R. A. (1979). Estimates of income for small places: an application of james-stein procedures to census data. *Journal of the American Statistical Association*, 74(366a):269–277.
- Finley, A. O. (2025). *Models for zero-inflated data*. Available at https://github.com/finleya/zi_models.

- Finley, A. O., Andersen, H.-E., Babcock, C., Cook, B. D., Morton, D. C., and Banerjee, S. (2024). Models to support forest inventory and small area estimation using sparsely sampled lidar: A case study involving g-liht lidar in tanana, alaska. *Journal of Agricultural, Biological and Environmental Statistics*, 29(4):695–722.
- Finley, A. O., Banerjee, S., and MacFarlane, D. W. (2011). A hierarchical model for quantifying forest variables over large heterogeneous landscapes with uncertain forest areas. *Journal of the American Statistical Association*, 106(493):31–48.
- Finley, A. O., Datta, A., Cook, B. D., Morton, D. C., Andersen, H. E., and Banerjee, S. (2019). Efficient algorithms for Bayesian nearest neighbor Gaussian processes. *Journal of Computational and Graphical Statistics*, 28(2):401–414.
- Gelman, A., Carlin, J., Stern, H., Dunson, D., Vehtari, A., and Rubin, D. (2013). *Bayesian Data Analysis, Third Edition*. Chapman & Hall/CRC Texts in Statistical Science. Taylor & Francis.
- May, P., McConville, K. S., Moisen, G. G., Bruening, J., and Dubayah, R. (2023). A spatially varying model for small area estimates of biomass density across the contiguous united states. *Remote Sensing of Environment*, 286:113420.
- Pfeffermann, D., Terryn, B., and Moura, F. (2008). Small area estimation under a two-part random effects model with application to estimation of literacy in developing countries. *Survey Methodology*, 34.
- Picotte, J. J., Dockter, D., Long, J., Tolk, B., Davidson, A., and Peterson, B. (2019). LANDFIRE remap prototype mapping effort: Developing a new framework for mapping vegetation classification, change, and structure. *Fire*, 2(2):35.
- Prisley, S., Bradley, J., Clutter, M., Friedman, S., Kempka, D., Rakestraw, J., and Sonne Hall, E. (2021). Needs for small area estimation: Perspectives from the us private forest sector. *Frontiers in Forests and Global Change*, 4:746439.

- R Core Team (2024). *R: A Language and Environment for Statistical Computing*. R Foundation for Statistical Computing, Vienna, Austria.
- Rao, J. and Molina, I. (2015). *Small Area Estimation*. Wiley, 2nd edition. ISBN: 978-1-118-73578-7.
- Rollins, M. G. (2009). LANDFIRE: a nationally consistent vegetation, wildland fire, and fuel assessment. *International Journal of Wildland Fire*, 18(3):235–249.
- Shannon, E. S., Finley, A. O., Domke, G. M., May, P. B., Andersen, H.-E., Gaines III, G. C., and Banerjee, S. (2024). Toward spatio-temporal models to support national-scale forest carbon monitoring and reporting. *Environmental Research Letters*, 20(1):014052.
- U.S. Geological Survey (2019). LANDFIRE Elevation.
- U.S. Senate (2023). *S. Rep. 118-83 - Department of the Interior, Environment, and Related Agencies Appropriations Bill*.
- White, G. W., Wieczorek, J. A., Cody, Z. W., Tan, E. X., Chistolini, J. O., McConville, K. S., Frescino, T. S., and Moisen, G. G. (2024a). Assessing small area estimates via bootstrap-weighted k-nearest-neighbor artificial populations.
- White, G. W., Wieczorek, J. A., Frescino, T. S., and McConville, K. S. (2024b). *kbaabb: Generates an Artificial Population Based on the KBAABB Methodology*. R package version 0.0.0.9000.
- White, G. W., Yamamoto, J. K., Elsyad, D. H., Schmitt, J. F., Korsgaard, N. H., Hu, J. K., Gaines, G. C., Frescino, T. S., and McConville, K. S. (2025). Small area estimation of forest biomass via a two-stage model for continuous zero-inflated data. *Canadian Journal of Forest Research*, 55:1–19.
- Wiener, S. S., Bush, R., Nathanson, A., Pelz, K., Palmer, M., Alexander, M. L., Anderson, D., Treasure, E., Baggs, J., and Sheffield, R. (2021). United states forest service use of

forest inventory data: Examples and needs for small area estimation. *Frontiers in Forests and Global Change*, 4:763487.

Yamamoto, J., Elsyad, D., White, G., Schmitt, J., Korsgaard, N., McConville, K., and Hu, K. (2025). *saeczi: Small Area Estimation for Continuous Zero Inflated Data*. R package version 0.2.0.9000, commit f580319049b152c890033c770913b7a296ce63cb.

Yang, L., Jin, S., Danielson, P., Homer, C., Gass, L., Bender, S. M., Case, A., Costello, C., Dewitz, J., Fry, J., Funk, M., Granneman, B., Liknes, G. C., Rigge, M., and Xian, G. (2018). A new generation of the United States National Land Cover Database: Requirements, research priorities, design, and implementation strategies. *ISPRS Journal of Photogrammetry and Remote Sensing*, 146:108–123.

Appendix

A Prior distributions and hyperparameters

Table 4 includes the prior distribution and hyperparameter values for all parameters used for the Bayesian models.

Parameter	Prior distribution	hyperparameter values
β_0	$\mathcal{N}(\mu, \sigma^2)$	$\mu = 0, \sigma^2 = 1000$
$\tilde{\beta}_0(\ell)$	$\mathcal{N}(\mu, \sigma^2)$	$\mu = 0, \sigma^2 = \sigma_{\tilde{\beta}_0}^2$
β_k	$\mathcal{N}(\mu, \sigma^2)$	$\mu = 0, \sigma^2 = 1000$
$\tilde{\beta}_{k,j}$	$\mathcal{N}(\mu, \sigma^2)$	$\mu = 0, \sigma^2 = \sigma_{\tilde{\beta}_{k,j}}^2$
$\sigma_{\tilde{\beta}_0}^2$	$\mathcal{IG}(a, b)$	$a = 2, b = 1$
$\sigma_{\tilde{\beta}_{k,j}}^2$	$\mathcal{IG}(a, b)$	$a = 2, b = 1$
$\varepsilon(\ell)$	$\mathcal{N}(\mu, \sigma^2)$	$\mu = 0, \sigma^2 = \tau^2$
τ^2	$\mathcal{IG}(a, b)$	$a = 2, b = 10$
α_0	$\mathcal{N}(\mu, \sigma^2)$	$\mu = 0, \sigma^2 = 1000$
$\tilde{\alpha}_0(\ell)$	$\mathcal{N}(\mu, \sigma^2)$	$\mu = 0, \sigma^2 = \sigma_{\tilde{\alpha}_0}^2$
α_k	$\mathcal{N}(\mu, \sigma^2)$	$\mu = 0, \sigma^2 = \sigma_{\alpha_k}^2$
$\sigma_{\tilde{\alpha}_0}^2$	$\mathcal{IG}(a, b)$	$a = 2, b = 1$
\mathbf{w}	$\mathcal{MVN}(\boldsymbol{\mu}, \boldsymbol{\Sigma})$	$\boldsymbol{\mu} = \mathbf{0}, \boldsymbol{\Sigma} = \sigma_w^2 \mathbf{R}(\phi)$
σ_w^2	$\mathcal{IG}(a, b)$	$a = 2, b = 1$
ϕ	$\mathcal{U}(a, b)$	$a = 0.003, b = 3$
$\varepsilon(\ell)$	$\mathcal{N}(\mu, \sigma^2)$	$\mu = 0, \sigma^2 = \tau^2$
$\varepsilon_1(\ell)$	$\mathcal{N}(\mu, \sigma^2)$	$\mu = 0, \sigma^2 = \tau_1^2$ or $\tau_{1,j}^2$
$\varepsilon_2(\ell)$	$\mathcal{N}(\mu, \sigma^2)$	$\mu = 0, \sigma^2 = \tau_2^2$
τ^2	$\mathcal{IG}(a, b)$	$a = 2, b = 10$
τ_1^2	$\mathcal{IG}(a, b)$	$a = 2, b = 10$
$\tau_{1,j}^2$	$\mathcal{IG}(a, b)$	$a = 2, b = 10$
τ_2^2	None	Set to 0.00001

Table 4: Prior distributions and hyperparameter values used for the Bayesian models.